frontiers | Frontiers in Plant Science

TYPE Original Research
PUBLISHED 14 November 2022
DOI 10.3389/fpls.2022.1062575

Check for updates

OPEN ACCESS

EDITED BY
Pengtao Ma,
Yantai University, China

REVIEWED BY
Long Li,
Chinese Academy of Agricultural Sciences (CAAS), China
Jihu Li,
SAAS, China

*CORRESPONDENCE
Junming Li
ljm@sjziam.ac.cn
Liqiang Song
songliqiang@hebau.edu.cn

†These authors have contributed equally to this work

SPECIALTY SECTION
This article was submitted to Plant Bioinformatics, a section of the journal Frontiers in Plant Science

RECEIVED 06 October 2022
ACCEPTED 24 October 2022
PUBLISHED 14 November 2022

CITATION
Liu J, Zhi L, Zhang N, Zhang W, Meng D, Batool A, Ren X, Ji J, Niu Y, Li R, Li J and Song L (2022) Transcriptomic analysis reveals the contribution of *QMrl-7B* to wheat root growth and development. *Front. Plant Sci.* 13:1062575. doi: 10.3389/fpls.2022.1062575

COPYRIGHT
© 2022 Liu, Zhi, Zhang, Zhang, Meng, Batool, Ren, Ji, Niu, Li, Li and Song. This is an open-access article distributed under the terms of the Creative Commons Attribution License (CC BY). The use, distribution or reproduction in other forums is permitted, provided the original author(s) and the copyright owner(s) are credited and that the original publication in this journal is cited, in accordance with accepted academic practice. No use, distribution or reproduction is permitted which does not comply with these terms.

Transcriptomic analysis reveals the contribution of *QMrl-7B* to wheat root growth and development

Jiajia Liu[1,2†], Liya Zhi[1,2†], Na Zhang[1], Wei Zhang[1], Deyuan Meng[1,2], Aamana Batool[1,2], Xiaoli Ren[1,2], Jun Ji[1], Yanxiao Niu[3], Ruiqi Li[4], Junming Li[1,3*] and Liqiang Song[4*]

[1]Center for Agricultural Resources Research, Institute of Genetics and Developmental Biology, Chinese Academy of Sciences, Shijiazhuang, Hebei, China, [2]The College of Life Science, University of Chinese Academy of Sciences, Beijing, China, [3]Ministry of Education Key Laboratory of Molecular and Cellular Biology, Hebei Collaboration Innovation Center for Cell Signaling, Hebei Key Laboratory of Molecular and Cellular Biology, College of Life Sciences, Hebei Normal University, Shijiazhuang, China, [4]State Key Laboratory of North China Crop Improvement and Regulation, College of Agronomy, Hebei Agricultural University, Baoding, Hebei, China

Roots are the major organs for water and nutrient acquisition and substantially affect plant growth, development and reproduction. Improvements to root system architecture are highly important for the increased yield potential of bread wheat. *QMrl-7B*, a major stable quantitative trait locus (QTL) that controls maximum root length (MRL), essentially contributes to an improved root system in wheat. To further analyze the biological functions of *QMrl-7B* in root development, two sets of *Triticum aestivum* near-isogenic lines (NILs), one with superior *QMrl-7B* alleles from cultivar Kenong 9204 (KN9204) named NIL^{KN9204} and another with inferior *QMrl-7B* alleles from cultivar Jing 411 (J411) named NIL^{J411}, were subjected to transcriptomic analysis. Among all the mapped genes analyzed, 4871 genes were identified as being differentially expressed between the pairwise NILs under different nitrogen (N) conditions, with 3543 genes expressed under normal-nitrogen (NN) condition and 2689 genes expressed under low-nitrogen (LN) condition. These genes encode proteins that mainly include NO_3^- transporters, phytohormone signaling components and transcription factors (TFs), indicating the presence of a complex regulatory network involved in root determination. In addition, among the 13524 LN-induced differentially expressed genes (DEGs) detected in this study, 4308 and 2463 were specifically expressed in the NIL^{KN9204} and NIL^{J411}, respectively. These DEGs reflect different responses of the two sets of NILs to varying N supplies, which likely involve LN-induced root growth. These

results explain the better-developed root system and increased root vitality conferred by the superior alleles of *QMrl-7B* and provide a deeper understanding of the genetic underpinnings of root traits, pointing to a valuable locus suitable for future breeding efforts for sustainable agriculture.

KEYWORDS

***Triticum aestivum*, root traits, RNA sequencing, differentially expressed gene, near-isogenic lines**

Introduction

Crops produce a large proportion of food and nutrients for humans in modern society. During the past 50 years, the application of chemical fertilizers and the Green Revolution have substantially increased crop production, maintaining food security for the increasingly growing population (Godfray et al., 2010). However, a continuous increase in crop output cannot sustainably be achieved by excessive amounts of fertilizer because of the limited nutrient use efficiency (NUE) of crop plants. Importantly, a large amount of wasted resources and environmental pollution resulting from excessive fertilizer applications cannot be ignored (Springmann et al., 2018). For these reasons, crop cultivars that have relatively high NUE are environmentally friendly and helpful to conserve resources for sustainable agriculture. Roots, the major organs for plant anchorage, nutrient and water absorption, and interactions with symbiotic organisms, have attracted increased amounts of attention in recent studies given the discovery of their correlations with nutrient use and crop yield (Gewin, 2010). In general, manipulation of root architecture traits, including root number, root length, root surface area (RA) and root volume (RV), especially the spatial configuration of the root system in the soil, is an essential approach to increase crop yields, which may represent an important component of a new green revolution (Lynch, 2007; Meister et al., 2014). Unfortunately, root traits have been chronically overlooked in the traditional breeding due to their lack of aboveground visibility (Maqbool et al., 2022).

Bread wheat (*Triticum aestivum* L.) is one of the most important crop species worldwide, providing ~20% of calories for human needs (Appels et al., 2018). Efforts have been made to explore the determinants of root traits that contribute to increase yield potential in wheat. In addition to traditional labor-intensive and time-consuming methods for root trait analysis (Kücke et al., 1995), artificial medium systems, such as hydroponic culture, have been used in many studies and revealed a series of quantitative trait loci (QTLs) that drive genetic variation in root traits (An et al., 2006; Cao et al., 2014; Kabir et al., 2015; Maccaferri et al., 2016; Merchuk-Ovnat et al., 2017; Fan et al., 2018; Zheng et al., 2019). However, it remains largely unclear of the mechanisms of these loci control root traits due to the complexity of the wheat genome. To date, a few genes regulating root morphology have been analyzed through reverse genetics studies in wheat. For example, the expressions of *TaRSL2* (Han et al., 2017a) and *TaLBD16* (Wang et al., 2018a) were shown to be positively correlated with root hair length and number of lateral roots, respectively. Heterogenous expressions of *TaMPK4* (Hao et al., 2015) and *TaMOR* (Li et al., 2016) demonstrated their positive effects on root development. Overexpression of the transcription factor (TF)-encoding genes *TaNAC2-5A* (He et al., 2015), *TaNFYA-B1* (Qu et al., 2015), *TaNAC69-1* (Chen et al., 2016) and *TaWRKY51* (Hu et al., 2018) resulted in enhanced root growth, while *TabZIP60* (Yang et al., 2019) had the opposite effects, implying a complex genetic basis of the formation of root traits. In addition, circular RNAs have been shown to participate in root length regulation (Xu et al., 2019).

At present, a holistic view of the root growth regulatory network and how it affects root traits and yield potential is strongly needed for molecular breeding. RNA sequencing (RNA-seq) makes it possible to explore the consistency between root morphology and its underlying mechanisms at the whole-plant level through DEG analysis. For example, the transcriptomic analysis revealed how the root growth of salt-tolerant bermudagrass was maintained under salinity stress; the salt tolerance was attributed to appropriate expression levels of genes involved in reactive oxygen species (ROS) homeostasis and cell wall loosening, which were regulated in part by a number of TFs linked to stress responses and growth regulation (Hu et al., 2015). DEGs detected in maize cultured under different nitrogen (N) levels highlighted the network of root growth in response to N deficiency, where the *LBD* TF-encoding gene participated in the balance between nutrient metabolism and the stress response (He et al., 2016). RNA-seq data suggested crosstalk occurs among the roots (in terms of

Abbreviations: NN, normal-nitrogen; LN, low-nitrogen; NIL, near-isogenic line; DEG, differentially expressed gene; QTL, quantitative trait locus; RNA-seq, RNA sequencing; NUE, nitrogen use efficiency; MRL, maximum root length; TRL, total root length; RA, root surface area; RV, root volume; GO, Gene Ontology; KEGG, Kyoto Encyclopedia of Genes and Genomes.

growth promotion), gibberellin (GA) biosynthesis, auxin signaling, cell division and cell wall modification in uniconazole-treated soybean (Han et al., 2017b). These findings enriched our understanding of the molecular mechanisms behind the interplay of root traits and other agronomic characteristics, helping to generate strategies for crops with improved root systems, increased NUE and improved environmental adaptation.

Previous studies have shown that *Triticum aestivum* KN9204has a larger root system than does cultivar J411 (Wang et al., 2011). Using a RIL population derived from the cross of KN9204 and J411 (KJ-RIL), researchers identified *QMrl-7B* as a major stable QTL that controls maximum root length (MRL) (Fan et al., 2018), and its contribution to large root systems was dissected (Liu et al., 2021), prompting the question of how *QMrl-7B* regulates root architecture and N uptake. In the present study, transcriptomic analysis of the pairwise *QMrl-7B* NILs was performed to further analyze the function of *QMrl-7B* in root development. The results will help reveal the pathways controlling root development that are affected by *QMrl-7B* in wheat, providing insights into the genetic and physiological basis underlying desirable root traits for agriculture.

Materials and methods

Plant materials and root phenotyping

KN9204 is a representative cultivar released in 2003 with a prolific root system, and J411 is a major cultivar that has been planted in the Northern China Plain since 1990s (Wang et al., 2011). Two sets of *QMrl-7B* NILs, one with superior alleles from KN9204 (referred to as the NIL^{KN9204}) and another with inferior alleles from J411 (referred to as the NIL^{J411}) (Liu et al., 2021), were used in this study for transcriptomic analysis.

The root morphological traits of the pairwise *QMrl-7B* NILs were characterized in the experiments involving different N hydroponic cultures, with three replications. Seeds were imbibed in distilled water at 23°C for 24 h and then transferred to plastic pots containing moist vermiculite and nutrient-enriched soil (1:1, v/v) for ten days. Uniform seedlings (at the one- and half-leaf stages) were then chosen, after which their residual endosperm was removed; they were subsequently cultured in both normal-nitrogen (NN) and low-nitrogen (LN) nutrient solutions as described by Fan et al. (2018). On the fourteenth (four-leaf stage) and twenty-first (five-leaf stage) days in different N hydroponic cultures, five uniform seedlings of each NIL were evaluated for their average MRL (cm), total root length (TRL, cm), RA (cm^2) and RV (cm^3). MRL was measured using a ruler, and the remaining traits (TRL, RA and RV) were quantified by using a ScanMaker i800 Plus Scanner (600 DPI) and analyzed by LA-S software (Hangzhou Wanshen Detection Technology Co., Ltd., Hangzhou, China; https://www.wseen.com).

Moreover, the roots of the four-leaf-stage seedlings of the pairwise NILs were sampled and immediately frozen in liquid N for subsequent RNA extraction. The root samples were divided into four treatments: the NIL^{KN9204} under NN condition (NN_NIL^{KN9204}), the NIL^{J411} under NN condition (NN_NIL^{J411}), the NIL^{KN9204} under LN condition (LN_NIL^{KN9204}) and the NIL^{J411} under LN condition (LN_NIL^{J411}). Each sample pool comprised five individual seedlings, and all experiments were replicated three times.

Transcriptome analysis

RNA extraction and sequencing

Total RNA was extracted from the root samples using TRIzol Reagent (Plant RNA Purification Reagent for plant tissue, Invitrogen, USA) according to the manufacturer's instructions, and genomic DNA was removed using DNase I (TaKaRa, Beijing, China). The quantity, quality, and integrity of the extracted RNA were determined using an ND-2000 spectrophotometer (Thermo Fisher Scientific, MA, USA) and an Agilent 2100 Bioanalyzer (Agilent Technologies, Santa Clara, CA, USA). Only high-quality RNA samples (OD260/280 = 1.8~2.2, OD260/230 ≥ 2.0, RNA integrity number (RIN) ≥ 6.5, 28S:18S ≥ 1.0, RNA content > 1 μg) were used to construct a sequencing library. Messenger RNA (mRNA) was isolated from the total RNA using magnetic beads with oligo (dT) primers and then cut into short fragments in a fragmentation buffer. Complementary DNA (cDNA) was subsequently synthesized using a SuperScript Double-Stranded cDNA Synthesis Kit (Invitrogen, CA, USA), with random hexamer primers (Illumina). The synthesized cDNA was then subjected to end repair, phosphorylation and polyadenylation according to Illumina's library construction protocol. The libraries were size selected for cDNA target fragments of 300 bp on 2% low-range ultra-agarose followed by PCR amplification using Phusion DNA polymerase (NEB); fifteen PCR cycles were performed. After quantification by a TBS-380 fluorometer, the paired-end RNA-seq library was sequenced with an Illumina HiSeq Xten/NovaSeq 6000 sequencer (2 × 150 bp read length). The library was then sequenced using the Illumina HiSeq™ platform (Shanghai Majorbio Bio-pharm Technology Co., Ltd., Shanghai, China).

Analysis of DEGs

The data were analyzed on the free online platform of the Majorbio Cloud Platform (https://www.majorbio.com). To obtain high-quality reads, reads containing adapter sequences and reads of low quality were removed from the raw data to obtain clean reads in FASTQ format. Q20 and Q30 values and GC contents were determined according to conventional

methods. Afterwards, the remaining clean reads were mapped to the reference genome of Chinese Spring (CS) (http://plants.ensembl.org/Triticum_aestivum/Info/Index/) by HISAT2 software (http://ccb.jhu.edu/software/hisat2/index.shtml). Unigene expression levels were estimated according to their transcripts per million reads mapped (TPM) values. DEGs between the NIL^{KN9204} and the NIL^{J411} under both NN and LN conditions were then analyzed using the DESeq2 package (Love et al., 2014), and the expression results are presented in terms of the log_2fold change (FC). $|log_2FC| \geq 1$ and p-adjusted< 0.05 were used as thresholds to judge the significance of gene expression differences. DEGs were also evaluated in response to LN stress for each NIL.

The DEGs of each one-to-one comparison were analyzed by Gene Ontology (GO) and Kyoto Encyclopedia of Genes and Genomes (KEGG) pathway enrichment analysis. GO functional enrichment and KEGG pathway analysis were carried out by Goatools (https://github.com/tanghaibao/Goatools) and KOBAS (http://kobas.cbi.pku.edu.cn/home.do), where GO terms and biological pathways with a p-adjusted< 0.05 were considered significantly enriched. The encoded products of the DEGs were subsequently annotated by the NCBI non-redundant protein (NR) database.

Quantitative real-time polymerase chain reaction validation

To confirm the reliability of the DEGs obtained from RNA-seq, eight DEGs on chromosome 7B were selected for qRT-PCR analysis. Gene-specific primers were designed using Primer Premier 5.0 software (Premier Biosoft International); the sequences are shown in Table S1. qRT-PCR was carried out in total volumes of 20 μl using a SYBR PCR kit (TaKaRa, Beijing, China) on an ABI 7500 real-time PCR system (Applied Biosystems, MA, USA) according to the manufacturers' instructions. Each sample was analyzed as three technical replicates, and the relative expression value of the DEGs was determined using the comparative cycle threshold (Ct) method after normalization to the expression of the GAPDH control.

Results

Root traits of the pairwise NILs

The root traits of the seedlings in hydroponic cultures with different N contents were evaluated. On the fourteenth day after the seedlings were transferred to the nutrient solutions, the average MRL, TRL, RA and RV of the four-leaf-stage NIL^{KN9204} seedlings were 22.28 cm, 255.77 cm, 25.47 cm^2 and 0.25 cm^3, respectively, under NN condition, which were significantly greater than those of the NIL^{J411} (19.85 cm, 203.47 cm, 20.64 cm^2 and 0.20 cm^3, respectively) under comparable conditions. Accordingly, the average MRL, TRL, RA and RV of the NIL^{KN9204} *vs* NIL^{J411} at the seedling stage were 28.07 *vs* 21.54 cm, 301.75 *vs* 282.12 cm, 27.28 *vs* 24.90 cm^2 and 0.25 *vs* 0.21 cm^3, respectively, under LN condition, indicating that the NIL^{KN9204} was superior to the NIL^{411} by 30.32%, 6.96%, 9.56% and 19.05%, respectively (p< 0.05). Notably, the MRL of the NIL^{KN9204} seedlings under LN condition was 25.99% greater than that under NN conditions, while only an 8.51% difference was recorded for the NIL^{411} under the hydroponic cultures with different N contents, indicating that LN more strongly induced the growth of primary roots for the NIL^{KN9204} than for the NIL^{411} (Figure 1). Similar change trends of MRL, TRL, RA and RV differences in the five-leaf-stage seedlings were also observed between the two sets of NILs at twenty-one days after the 10-day-old seedlings were transferred to the nutrient solutions (Figure S1). Taken together, the above results showed that, in comparison to the NIL^{411}, the NIL^{KN9204} had superior root architecture characteristics during the seedling stage, especially under LN condition.

Overview of transcriptome sequencing results

To explore the genetic and physiological basis of the superior root traits of the NIL^{KN9204}, roots of four-leaf-stage seedlings of the pairwise NILs cultured under both NN conditions and LN conditions were sampled for transcriptomic analysis. RNA-seq on the Illumina HiSeq™ platform (http://www.majorbio.com) generated 70576620~90524786 clean reads per sample, with a sequencing error of less than 0.3%. The average Q20, Q30 and GC content percentages were 97.06%, 92.27% and 53.98%, respectively. These findings attest to the fine quality of the sequencing results. Mapping of the reads with the Chinese Spring (CS) reference genome revealed an alignment in a range of 81.48~90.35%, among which 76.14~84.54% of the genes were uniquely mapped and 5.34~6.28% were multiply mapped (Table S2). The correlation coefficient of repeats ranged from 0.69~0.98 (Figure S2, Table S3). These data were deemed suitable for subsequent analysis (Table S4), in which the DEGs whose expression was upregulated ($log_2FC \geq 1$) and downregulated ($log_2FC \leq -1$) in each one-to-one comparison were statistically (p-adjusted< 0.05) analyzed.

Identification of DEGs between the pairwise NILs

The transcriptomic changes in the roots between the pairwise *QMrl-7B* NILs were compared under both NN and LN conditions. Under NN condition, a total of 3543 genes were differentially expressed between the two sets of NILs, of which

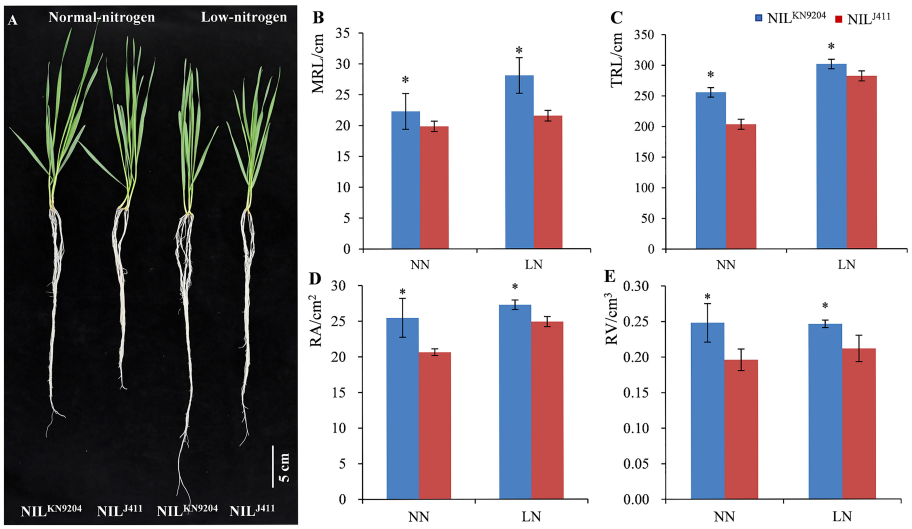

FIGURE 1
Phenotypes of four-leaf-stage seedlings **(A)** and the corresponding root traits **(B-E)** of the pairwise NILs cultured in nutrient solutions with different N contents for fourteen days NN and LN indicate normal- and low-nitrogen conditions, respectively. MRL, TRL, RA and RV indicate the maximum root length, total root length, root surface area and root volume, respectively. "*" indicates a significant difference at $p < 0.05$.

the expression of 1045 genes was upregulated and that of 2498 was downregulated in the NIL^{KN9204} (Figure 2A; Table S5). These genes were enriched in 320 subcategories according to GO analysis, of which 200, fourteen and 106 belonged to biological processes, cellular components and molecular functions, respectively, and the three most enriched biological processes were "biological process (GO:0008150)", "metabolic process (GO:0008152)" and "phosphate-containing compound metabolic process (GO:0006796)" (Table S6). "Phenylpropanoid biosynthesis (map00940)" was the most enriched pathway according to KEGG analysis (Table S7). Under the LN condition, 2689 genes were differentially expressed between the pairwise NILs, including 990 genes whose expressions were upregulated and 1699 genes whose expressions were downregulated in the NIL^{KN9204} (Figure 2A; Table S8). These DEGs were categorized into biological process (141), cellular component (12) and molecular function (77) categories by GO analysis. The three most enriched biological processes were "biological process (GO:0008150)", "metabolic process (GO:0008152)" and "phosphate-containing compound metabolic process (GO:0006796)" (Table S9). Similarly, "phenylpropanoid biosynthesis (map00940)" was the most enriched pathway according to the KEGG analysis (Table S10).

Notably, there were 315 DEGs whose expressions increased and 1034 DEGs whose expressions decreased in the NIL^{KN9204} compared to the NIL^{J411} simultaneously under both NN and LN conditions (Figure 2A). These genes might participate in translation, transcriptional regulation and cycle control according to GO and KEGG enrichment analysis (Figure 2B; Tables S11-S13), reflecting the permanent effects of the *QMrl-7B* locus that were not affected by N levels. Under NN condition, nine genes were expressed at higher levels in the NIL^{KN9204} than in the NIL^{J411}; however, these genes were expressed at a higher level in the NIL^{J411} under LN condition (Figure 2A; Table 1). In addition, three genes exhibited the opposite expression trend, implying their functional difference in response to N stress (Figure 2A; Table 1).

Identification of DEGs in response to N deficiency

The differences in DEGs in the root response to N deficiency between the NIL^{KN9204} and NIL^{J411} were analyzed. Compared with the NN condition, LN condition yielded 11073 DEGs (6341 whose expression increased and 4732 whose expression decreased) and 9228 DEGs (5072 whose expression increased and 4156 whose expression decreased) in the $NIL^{KN9204}$and NIL^{J411}, respectively (Figure 3A). A total of 2385 DEGs whose expressions increased and 1923 DEGs whose expressions decreased were detected only in the NIL^{KN9204} (Figure 3A; Table S14), whereas 1116 DEGs whose expressions increased and 1347 DEGs whose expressions decreased were detected specifically in the NIL^{J411} (Figure 3A; Table S17). Interestingly, there were more genes whose expressions were upregulated than genes whose expressions were downregulated in the NIL^{KN9204}, and the opposite trend occurred in the NIL^{J411}. GO analysis showed that these DEGs participate in multiple processes, and "phenylpropanoid biosynthesis (map00940)" was the most enriched process according to KEGG analysis (Figures 3B, C;

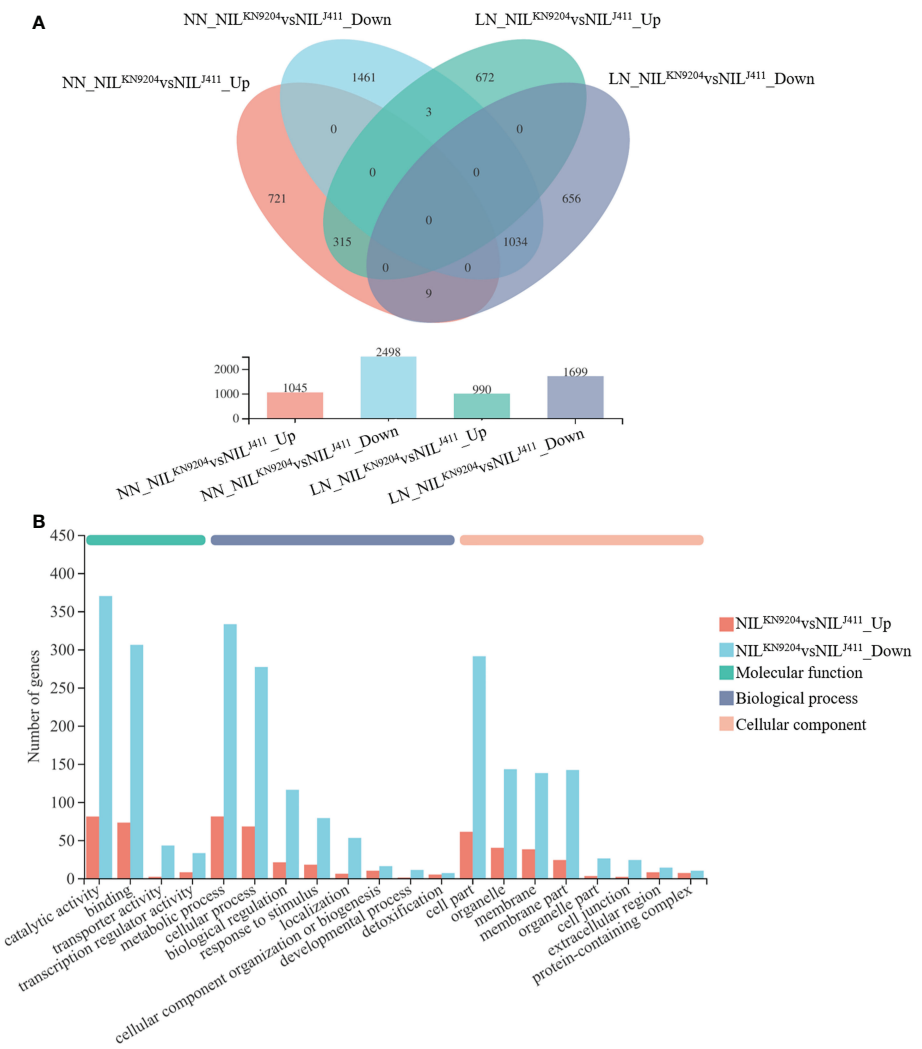

FIGURE 2
Identification of DEGs between the pairwise NILs NN and LN indicate normal- and low-nitrogen conditions, respectively. The expression levels between the NIL^{KN9204} and the NIL^{J411} were compared under each condition, with the former as a control. NIL^{J411}*vs*NIL^{KN9204}_Up and NIL^{J411}*vs*NIL^{KN9204}_Down indicate DEGs whose expression was upregulated and downregulated in the NIL^{J411} compared to the NIL^{KN9204} under the same culture conditions, respectively. **(A)** Venn diagram analysis of DEGs in each one-to-one comparison between the pairwise NILs under both NN and LN conditions. **(B)** GO annotation analysis of DEGs between the pairwise NILs that were simultaneously expressed under both NN and LN conditions with the first 20 terms as indicated.

Tables S14-S19). The expression of genes that differed specifically in the NIL^{KN9204} or the NIL^{J411} might give rise to a specific N response related to *QMrl-7B*, while a large number of common DEGs (3956 genes whose expression was upregulated and 2809 genes whose expression downregulated) in the two sets of NILs reflected the general response to N stress in wheat.

Quantitative real-time PCR verification

qRT-PCR analysis revealed that the expression levels of eight randomly selected DEGs on chromosome 7B were significantly different between the NIL^{KN9204} and the NIL^{J411} under NN conditions and LN conditions (Figure 4). These results nearly matched the expression profiles revealed by RNA-seq, confirming the results of the transcriptome sequencing of the pairwise NILs cultured under both NN and LN conditions.

Discussion

Improving plant roots is an effective way to increase NUE and minimize fertilizer application for sustainable agricultural development (Lynch, 2007). A number of genes/QTLs have been

TABLE 1 DEGs with opposite expression patterns between the pairwise NILs under NN and LN conditions.

Gene_ID	log_2FC (NN_NIL^{KN9204}/ NN_NIL^{J411})	*p*-adjusted	log_2FC (LN_NIL^{KN9204}/ LN_NIL^{J411})	*p*-adjusted	NR_description
TraesCS2A02G399900	1.07	0.002	-1.97	7.77E-20	MATE efflux family protein 9
TraesCS2B02G125500	-1.37	0.0098	1.08	1.25E-06	class III peroxidase
TraesCS2B02G626400	-5.11	2.88E-34	1.11	2.48E-05	probable 1-deoxy-D-xylulose-5-phosphate synthase 2, chloroplastic
TraesCS3B02G448000	1.74	1.07E-18	-1.35	1.98E-06	unnamed protein product
TraesCS3D02G094500	-2.06	5.54E-07	1.68	0.001	MYB-related protein 305-like
TraesCS3D02G225500	1.16	0.0002	-1.42	4.08E-14	uncharacterized protein LOC109770081
TraesCS3D02G408000	1.21	2.62E-07	-1.68	4.76E-16	BTB/POZ and TAZ domain-containing protein 2-like
TraesCS4A02G286600	1.32	4.98E-05	-1.73	2.50E-10	uncharacterized protein LOC109755115
TraesCS4B02G078800	1.85	3.67E-15	-1.07	5.58E-06	hypothetical protein TRIUR3_28321
TraesCS4D02G025500	1.18	0.0003	-1.97	2.85E-08	uncharacterized protein LOC109755115
TraesCS6B02G044300	1.15	0.001	-1.47	4.78E-08	high-affinity nitrate transporter TaNRT2
TraesCS6D02G035900	1.01	0.016	-1.02	0.002	high-affinity nitrate transporter 2.1-like

NN and LN indicate normal- and low-nitrogen conditions, respectively. AA and BB indicate the NIL^{KN9204} and the NIL^{J411}, respectively. The expression levels between the NIL^{KN9204} and the NIL^{J411} were compared under each condition, with the latter as a control. The expression ratios are presented as log_2FC values. Genes with a $log_2FC \leq -1$ (p-adjusted< 0.05, coloured blue) represent the genes whose expression was downregulated in the NIL^{KN9204}, and genes with $log_2FC \geq 1$ (p-adjusted< 0.05, coloured red) represent the genes whose expression was upregulated in the NIL^{KN9204}.

reported to be related to root growth and development; as such, these genes/QTLs have potential application in crop genetic improvement (Zhuang et al., 2021; Chen et al., 2022; Li et al., 2022). However, the genetic network explaining how these genes interact to influence root architecture still needs to be elucidated to assess the beneficial agronomic traits from an overall perspective and to guide the use of beneficial genes or pyramid of allelic variation in future breeding efforts. Compared with J411, KN9204 had a larger root system (Wang et al., 2011), with which the stable QTL *QMrl-7B* was associated (Fan et al., 2018). Further studies involving *QMrl-7B* NILs showed that, as compare to the NIL^{J411}s, the NIL^{KN9204}s had superior root traits, N-related traits and yield traits in field trials (Liu et al., 2021). The superiority of root traits of the NIL^{KN9204} at the seedling stage was also consistently proven in the present study. When these hydroponically cultured pairwise NILs were used for transcriptomic analysis, it was found that the DEGs detected by RNA-seq encoded proteins of various groups, such as transporters, enzymes, TFs, and components involved in hormone signaling. The important DEGs that might be involved in root trait regulation are discussed here.

The genes with opposite expression patterns between the pairwise NILs under the NN and LN conditions were very likely to be involved in N-related root growth (Tables 1, S5 and S8). For example, the expression level of the class III peroxidase gene (*TraesCS2B02G125500*) was higher in the NIL^{J411} under NN condition but was higher in the NIL^{KN9204} under LN condition. Class III peroxidase uses H_2O_2 as a substrate to produce OH^- radicals that enhance cell wall plastic extensibility and elongation by nonenzymatic cleavage of cell wall polysaccharides (Cosio and Dunand, 2009). Since root development is directly related to cell wall loosening and elongation, the upregulated expression of this gene by LN in the NIL^{KN9204} (Table S14) was proposed to participate in LN-promoted root growth by affecting these processes. Another most enriched process of the DEGs between the pairwise NILs was phenylpropanoid biosynthesis that might affect root enlargement (Muro-Villanueva et al., 2019; Liu et al., 2020). Interestingly, the expression levels of a series of phenylalanine ammonia-lyase and cinnamoyl-CoA reductase genes increased in the NIL^{J411} under both NN and LN conditions (Tables S5 and S8), implying that the biosynthesis of cinnamate and lignin monomers increased, which cannot directly explain the reason for the smaller roots.

Nitrate is substantially absorbed and transported by high-affinity (NRT2s) and low-affinity (NPFs) nitrate transporters for assimilation and storage (Xu et al., 2012; Wang et al., 2018b). N stress tolerant sorghum genotypes exhibit higher expression levels of high-affinity NRTs than do the sensitive genotypes under N-limiting conditions (Gelli et al., 2014). We previously compared the expression profiles of 44 NRT2 and 217 NPF genes in the roots of KN9204 and J411 cultivated hydroponically with and without N supply and found that up to 79.2% and 43.7% of the root-expressed NRT2 and NPF genes, respectively, displayed differential expression between KN9204 and J411. Under NN conditions, more than two-thirds of the differentially expressed NRT2 and NPF genes exhibited higher expression in KN9204 than in J411, but the proportion of NRT2 and NPF genes with higher expression levels in KN9204 decreased under LN treatment, as the upregulated expression levels of most nitrate transporter genes, NRT2 family in particular, were higher in J411 than in KN9204 (Shi et al.,

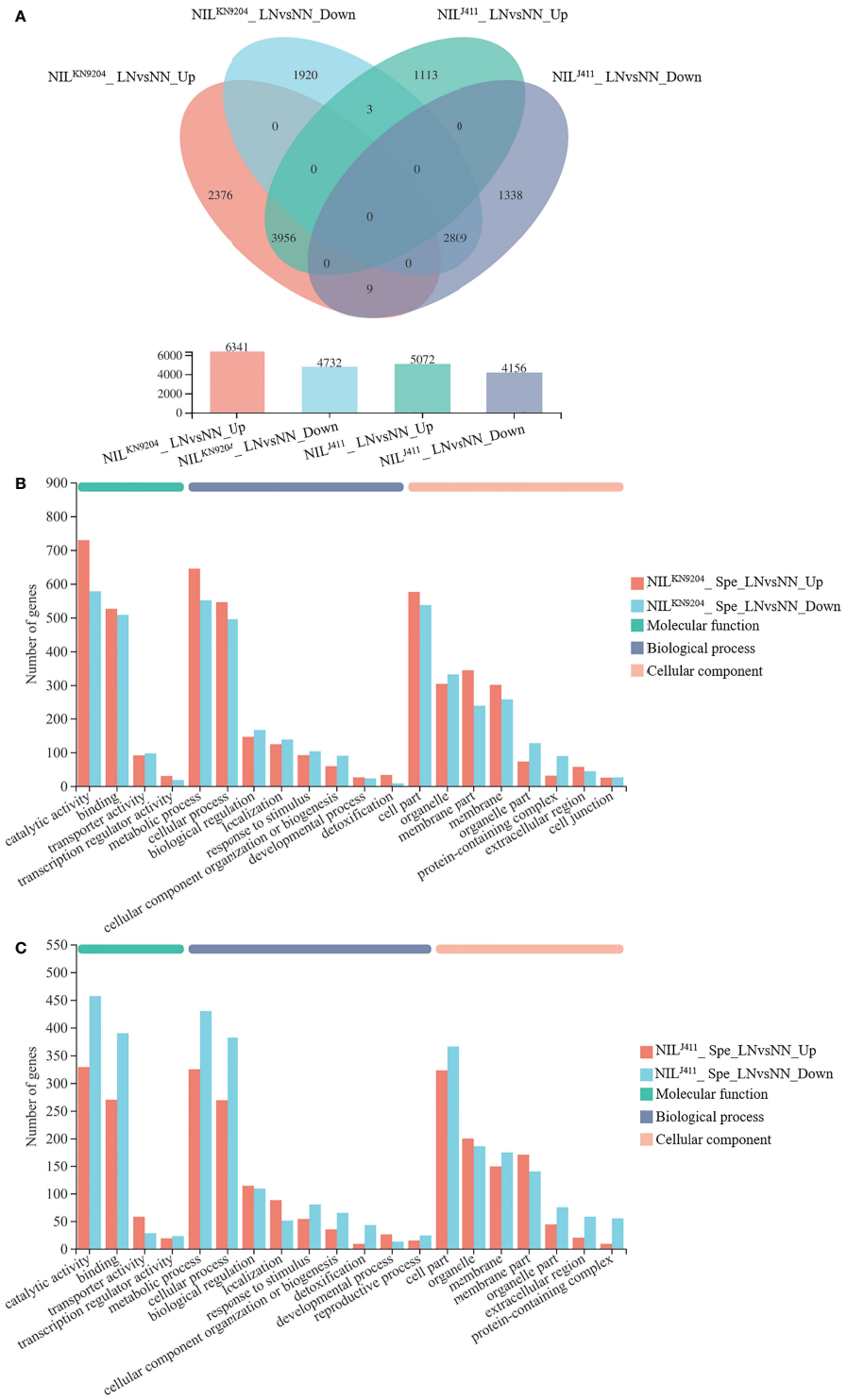

FIGURE 3
Identification of DEGs induced by LN NN and LN indicate normal- and low-nitrogen conditions, respectively. Spe indicates DEGs specifically expressed in the NIL^{KN9204} or the NIL^{J411}. The expression levels between NN and LN conditions were compared for each NIL, with NIL^{KN9204} as a control. LNvsNN_Up and LNvsNN_Down indicate DEGs whose expression was upregulated and downregulated under LN compared to NN for the same NIL. **(A)** Venn diagram analysis of the DEGs in each one-to-one comparison between NN and LN conditions for both the NIL^{KN9204} and NIL^{J411}. **(B, C)** GO annotation analysis of the genes whose expression differed specifically in the NIL^{KN9204}**(B)** and NIL^{J411} **(C)** with the first 20 terms as indicated.

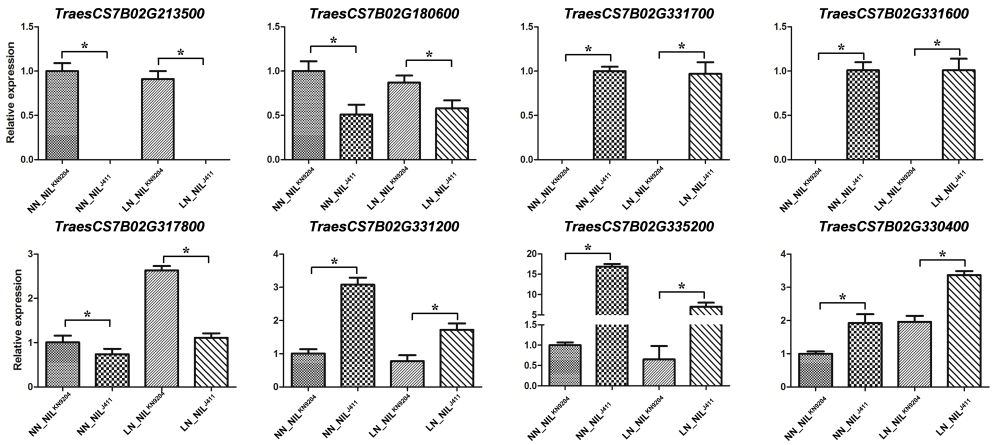

FIGURE 4
Validation of gene expression by qRT-PCR The relative mRNA expression of eight representative genes was checked by qRT-PCR. Each bar shows the mean ± standard error of three biological replicates. "*" indicates a significant difference at $p < 0.05$.

2022). Similarly, two high-affinity NRT genes (*TraesCS6B02G044300* and *TraesCS6D02G035900*) exhibited lower expression levels in the NIL^{J411} under NN condition, but higher expression levels in the NIL^{J411} than in the NIL^{KN9204} under LN condition (Table 1). In addition, the expressions of four high-affinity NRT genes (*TraesCS6A02G031000*, *TraesCS6A02G031100*, *TraesCS6B02G044100* and *TraesCS6B02G044500*) were induced specifically by LN in the NIL^{J411} but not in the NIL^{KN9204} (Table 2). Our present study showed that LN led to altere expression of a number of genes encoding both low-affinity and high-affinity NRTs (Table S4), in accordance with the viewpoint that different NRTs function at different N levels (Zhang and Forde, 1998).

Dual-affinity nitrate transporter 1 (NRT1) not only functions in N acquisition but also is a NO_3^- sensor; this action is independent of its uptake activity that controls root development (Ho et al., 2009). The cotransport of NO_3^-, peptides and hormones through the NRT1 family of transporters implies the occurrence of crosstalk between NO_3^- and other signaling pathways (Krouk et al., 2010; Tal et al., 2016). In our study, the expression levels of two and eleven putative NRT1 genes in the NIL^{KN9204} were higher and lower than those in the NIL^{J411} under both NN and LN conditions (Table 3), respectively, indicating that the differences in root traits may result mainly from NRT1 functional differentiation. Additionally, the higher expression level of the CBL-interacting protein kinase 23 (CIPK23) gene (*TraesCS2A02G251800*) in the NIL^{J411} compared to the NIL^{KN9204} was also independent of N status (Tables S5 and S8); this phenomenon may affect root formation together with NRT1 by phosphorylating T101 to regulate its primary NO_3^- response and high-affinity NO_3^- transport (Ho et al., 2009). Taken together, these results implied that a more sensitive response of roots to N acquisition occurred in the NIL^{J411} compared with the NIL^{KN9204}, which cannot be fully explained.

Phytohormones, together with their receptors and signaling components, constitute the main intrinsic regulatory pathways of root traits. Ethylene, whose biosynthesis is regulated by several key enzymes, such as 1-aminocyclopropane-1-carboxylic acid (ACC) synthase (ACS) and ACC oxidase (ACO), usually plays a negative regulatory role in root growth, inhibiting root enlargement and root meristem cell proliferation (Pattyn et al., 2020). In addition, ethylene regulates the expression of glutathione S-transferase (GST)-encoding genes. GST catalyses the conjugation of glutathione to various electrophilic compounds involved in the oxidative stress response, crosstalk with other hormones and drought-induced root growth (Dalal et al., 2018). Under both NN and LN conditions, significant increases in expression levels of genes encoding ACOs and GSTs were detected in the NIL^{J411}, with parallel increases in expression levels of genes encoding ethylene-responsive TFs (Table 4), implying that enhanced ethylene signaling together with glutathione metabolism negatively regulated root growth in the NIL^{J411}. GA, whose catabolism is catalysed by GA2-oxidase, is considered a negative regulator of lateral root formation (Gou et al., 2010). However, overexpression of GA2-oxidase-encoding genes led to shortened primary root length, and mutations in these kinds of genes led to somewhat longer roots (Li et al., 2017), indicating a negative correlation between GA2-oxidase-encoding genes and root length. Compared to the NIL^{KN9204}, the NIL^{J411} displayed upregulated expression levels of several GA2-oxidase-encoding genes under both NN and LN conditions (Table 4); these upregulated levels may have inhibitory effects on root development. Brassinosteroids (BRs) regulate both root meristem size and cell expansion in controlling root growth.

TABLE 2 *NRT* genes specifically expressed in the NIL^{KN9204} or NIL^{J411} in response to LN.

Gene_ ID	log_2FC (LN_NIL^{KN9204}/ NN_NIL^{KN9204})	*p*-adjusted	log_2FC (LN_NIL^{J411}/ NN_NIL^{J411})	*p*-adjusted	NR_description
TraesCS1A02G150200	1.03	0.004	0.14	0.84	Peptide transporter PTR3-A
TraesCS1A02G150400	1.18	2.29E-07	0.64	0.08	protein NRT1/PTR FAMILY 5.2-like
TraesCS1B02G168100	1.60	1.11E-12	0.90	0.01	protein NRT1/PTR FAMILY 5.2-like
TraesCS1B02G225000	-1.39	2.12E-06	-0.14	0.81	protein NRT1/PTR FAMILY 6.3-like
TraesCS1B02G267900	1.29	0.01	1.15	0.18	protein NRT1/PTR FAMILY 3.1-like
TraesCS1D02G201100	1.13	2.34E-11	0.81	0.0004	uncharacterized protein LOC109744571
TraesCS1D02G214300	-1.47	7.24E-08	0.20	0.72	protein NRT1/PTR FAMILY 6.3-like
TraesCS2A02G007500	0.60	0.08	1.05	1.54E-09	protein NRT1/PTR FAMILY 8.5-like
TraesCS2A02G074800	-1.89	0.003	-0.58	0.45	high-affinity nitrate transporter 2.1-like
TraesCS2A02G264500	0.99	8.86E-05	1.06	0.0006	protein NRT1/PTR FAMILY 4.5-like
TraesCS2B02G277600	0.71	0.003	1.27	6.40E-09	protein NRT1/PTR FAMILY 4.5-like
TraesCS2B02G626000	1.02	1.30E-05	0.43	0.19	protein NRT1/PTR FAMILY 5.10-like
TraesCS2B02G626700	1.76	1.07E-08	0.97	0.01	protein NRT1/PTR FAMILY 5.10-like
TraesCS2D02G413900	1.50	0.02	1.74	0.08	protein NRT1/PTR FAMILY 8.2-like
TraesCS2D02G583500	0.99	0.01	1.30	0.0005	protein NRT1/PTR FAMILY 5.10-like
TraesCS3A02G382100	-2.55	6.06E-20	-0.94	0.34	protein NRT1/PTR FAMILY 5.1-like isoform X1
TraesCS3A02G382200	-0.12	0.90	1.57	0.003	unnamed protein product
TraesCS3B02G095900	0.20	0.62	1.12	0.02	unnamed protein product
TraesCS3B02G414900	-3.35	5.34E-07	0.20	0.90	unnamed protein product
TraesCS3B02G415700	0.81	0.12	1.01	0.02	predicted protein
TraesCS3D02G056700	0.85	0.25	1.43	0.048	protein NRT1/PTR FAMILY 8.2-like isoform X1
TraesCS4A02G225400	-1.07	6.53E-06	-0.97	0.007	protein NRT1/PTR FAMILY 4.3-like
TraesCS4A02G283900	1.20	6.27E-15	0.93	9.83E-06	protein NRT1/PTR FAMILY 2.11-like
TraesCS4D02G026800	1.01	1.57E-08	0.85	1.76E-05	protein NRT1/PTR FAMILY 2.11-like
TraesCS4D02G087900	-1.39	2.77E-07	-0.997	0.002	protein NRT1/PTR FAMILY 4.3-like
TraesCS5B02G039100	3.41	0.02	2.02	0.22	protein NRT1/PTR FAMILY 2.11-like
TraesCS5B02G152000	1.42	0.31	3.72	0.04	putative nitrate excretion transporter 3
TraesCS5B02G245300	2.48	8.76E-05	1.89	0.09	predicted protein
TraesCS5B02G393100	1.46	0.39	4.38	0.03	protein NRT1/PTR FAMILY 4.5-like
TraesCS5B02G414000	0.79	0.008	1.14	2.22E-05	protein NRT1/PTR FAMILY 6.4 isoform X2
TraesCS5B02G498700	-0.82	0.02	-1.09	0.01	protein NRT1/PTR FAMILY 5.6-like
TraesCS5D02G419200	0.89	0.03	1.91	0.0007	protein NRT1/PTR FAMILY 6.4 isoform X1
TraesCS5D02G498700	-1.03	0.009	-0.95	0.0004	protein NRT1/PTR FAMILY 5.6-like
TraesCS6A02G030700	-2.93	7.26E-18	-0.63	0.17	high-affinity nitrate transporter 2.1-like
TraesCS6A02G030800	-2.84	1.38E-27	-0.38	0.50	high-affinity nitrate transporter 2.1-like
TraesCS6A02G030900	-2.75	1.36E-29	-0.43	0.33	High-affinity nitrate transporter 2.1
TraesCS6A02G031000	0.20	0.78	1.63	0.0002	High-affinity nitrate transporter 2.1
TraesCS6A02G031100	0.01	0.98	1.45	3.00E-05	high affinity nitrate transporter
TraesCS6A02G033100	-6.88	4.09E-06	-2.71	1	high-affinity nitrate transporter 2.1-like
TraesCS6A02G033200	-6.79	8.35E-06	-3.36	1	High affinity nitrate transporter 2.4

(Continued)

TABLE 2 Continued

Gene_ ID	log_2FC (LN_NIL^{KN9204}/ NN_NIL^{KN9204})	*p*-adjusted	log_2FC (LN_NIL^{J411}/ NN_NIL^{J411})	*p*-adjusted	NR_description
TraesCS6A02G267700	0.30	0.62	-1.13	4.90E-05	protein NRT1/PTR FAMILY 8.3-like
TraesCS6A02G369900	4.75	0.01	0.22	0.93	protein NRT1/PTR FAMILY 8.3-like isoform X1
TraesCS6B02G044100	0.06	0.90	1.51	4.09E-05	high affinity nitrate transporter
TraesCS6B02G044200	-1.21	2.49E-05	0.42	0.39	high-affinity nitrate transporter 2.1-like
TraesCS6B02G044400	-1.37	6.30E-07	0.93	0.01	high-affinity nitrate transporter 2.1-like
TraesCS6B02G044500	0.17	0.72	3.46	2.47E-36	high affinity nitrate transporter
TraesCS6B02G309200	-1.09	0.10	-2.04	0.008	protein NRT1/PTR FAMILY 7.3-like
TraesCS6D02G035900	-2.25	6.07E-16	-0.22	0.69	high-affinity nitrate transporter 2.1-like
TraesCS6D02G037800	-3.88	0.02	-3.59	0.23	high-affinity nitrate transporter 2.1-like
TraesCS6D02G132100	1.45	0.008	1.18	0.09	protein NRT1/PTR FAMILY 8.3-like
TraesCS7A02G121600	1.87	4.14E-10	0.60	0.24	protein NRT1/PTR FAMILY 2.3-like
TraesCS7A02G301700	-1.26	5.33E-12	-0.96	3.48E-08	protein NRT1/PTR FAMILY 6.3-like
TraesCS7B02G262200	0.99	2.59E-05	1.16	2.16E-08	protein NRT1/PTR FAMILY 4.6-like
TraesCS7B02G283400	0.93	0.0001	1.31	0.0001	protein NRT1/PTR FAMILY 8.3-like
TraesCS7D02G049300	0.71	0.16	1.80	0.004	protein NRT1/PTR FAMILY 2.3-like
TraesCS7D02G357300	1.11	2.26E-06	0.83	0.0003	protein NRT1/PTR FAMILY 4.6-like

NN and LN indicate normal- and low-nitrogen conditions, respectively. AA and BB indicate the NIL^{KN9204} and the NIL^{J411}, respectively. The expression levels between the NIL^{KN9204} and the NIL^{J411} were compared under each condition, with the latter as a control. The expression ratios are presented as log_2FC values. Genes with a $log_2FC \leq -1$ (p-adjusted< 0.05, coloured blue) represent the genes whose expression was downregulated under LN conditions, and genes with $log_2FC \geq 1$ (p-adjusted< 0.05, coloured red) represent the genes whose expression was upregulated under LN conditions.

Deficiency or insensitivity of BRs leads to reduced root growth and lateral root formation (Wei and Li, 2016). The decreased expression of receptor-like protein kinase BRI1-like 3 genes in the NIL^{J411} might impair BR signaling and inhibited root enlargement (Table 4). Auxin facilitates lateral root initiation and development (Fukaki and Tasaka, 2009), while cytokinin antagonistically negatively regulates root growth (Moubayidin et al., 2009). In rice, crown root primordium initiation was promoted by auxin signaling, whereas cytokinin signaling inhibited it (Neogy et al., 2021). Members of the *GH3* gene family respond to auxin and their encoding products use various amino acids as substrates to form indole-acetic acid (IAA)-amido conjugates for temporary storage and degradation (Staswick et al., 2005). Arabidopsis *GH3.17* gene regulates environment-induced hypocotyl elongation (Zheng et al., 2016) and it is also responsible for root elongation, whereas gh3 mutants accumulate more free-IAA at the expense of any IAA-Glu and IAA-Asp auxin conjugates which causes defects in root development, demonstrating the critical roles of *GH3* genes in auxin homeostasis and plant development (Guo et al., 2022). Cytokinin is activated by phosphoribohydrolase, which catalyses the hydrolysis of the bond between N^6-substituted bases and ribose 5'-monophosphates in cytokinin precursors during its biosynthesis process (Kurakawa et al., 2007). Rice *GH3-8* gene functions as a repressor of auxin-dependent developmental signaling, overexpression of *GH3-8* suppressed auxin action, which resulted in abnormal morphology similar to that reported in auxin-deficient plants i.e. shorter roots and fewer adventitious roots (Ding et al., 2008). Significant increases in expression levels were observed for genes encoding GH3.8 and phosphoribohydrolase in the NIL^{J411}, accompanied by decreased expression levels of a gene encoding an auxin-responsive protein (Table 4), implying the presence of weakened auxin signaling and accelerated cytokinin flux in the NIL^{J411}, which may be related to the differences in root traits of the pairwise NILs.

Several types of TFs play essential roles in root growth by regulating the expression of downstream genes that are usually closely associated with nutrient acquisition. Overexpression of *TaNFYA-B1* was shown to increase both primary root length and total lateral root length in wheat (Qu et al., 2015). The expression levels of genes encoding NF-Y subunit C-3-like proteins (*TraesCS1A02G354900*, *TraesCS1B02G366800* and *TraesCS1D02G355600*) were higher in the NIL^{KN9204} than in the NIL^{J411} under LN condition (Table 5), indicating their potential contribution to LN-induced root enlargement. NAC

TABLE 3 Differentially expressed *NRT* genes between the pairwise NILs.

Gene_ ID	log_2FC (NN_NIL^{KN9204}/ NN_NIL^{J411})	*p*-adjusted	log_2FC (LN_NIL^{KN9204}/ LN_NIL^{J411})	*p*-adjusted	NR_description
TraesCS2A02G309100	-1.43	9.78E-12	-1.24	2.60E-12	protein NRT1/PTR FAMILY 4.3-like
TraesCS2A02G572200	1.13	0.04	1.20	0.003	protein NRT1/PTR FAMILY 5.10-like
TraesCS5A02G485200	-1.03	0.006	-1.12	0.01	protein NRT1/PTR FAMILY 5.6-like
TraesCS5D02G498700	-2.07	4.20E-15	-2.15	1.62E-11	protein NRT1/PTR FAMILY 5.6-like
TraesCS6A02G267600	-1.44	0.0001	-1.92	0.002	protein NRT1/PTR FAMILY 8.3-like
TraesCS6A02G267700	-3.00	1.90E-24	-1.56	6.45E-06	protein NRT1/PTR FAMILY 8.3-like
TraesCS6A02G267800	-3.23	3.26E-05	-2.90	0.006	protein NRT1/PTR FAMILY 8.3-like
TraesCS6A02G268500	-1.09	7.42E-05	-1.56	0.005	protein NRT1/PTR FAMILY 8.3-like
TraesCS6B02G295000	-2.41	1.52E-13	-2.40	5.56E-08	protein NRT1/PTR FAMILY 8.3-like
TraesCS6B02G295600	-1.85	1.83E-12	-1.78	0.005	protein NRT1/PTR FAMILY 8.3-like
TraesCS6D02G247000	-4.10	4.91E-25	-2.03	0.0001	protein NRT1/PTR FAMILY 8.3-like
TraesCS6D02G247100	-1.45	9.32E-05	-1.88	5.83E-05	protein NRT1/PTR FAMILY 8.3-like isoform X1
TraesCS7D02G378300	1.53	0.0004	1.04	0.008	protein NRT1/PTR FAMILY 8.3-like isoform X1

NN and LN indicate normal- and low-nitrogen conditions, respectively. AA and BB indicate the NIL^{KN9204} and the NIL^{J411}, respectively. The expression levels between the NIL^{KN9204}and the NIL^{J411} were compared under each condition, with the latter as a control. The expression ratios are presented as log_2FC values. Genes with a $log_2FC \leq -1$ (p-adjusted< 0.05, coloured blue) represent the genes whose expression was downregulated in the NIL^{KN9204}, and genes with $log_2FC \geq 1$ (p-adjusted< 0.05, coloured red) represent the genes whose expression was upregulated in the NIL^{KN9204}.

TABLE 4 DEGs involved in phytohormone metabolism and signaling between the pairwise NILs.

Gene_ ID	log_2FC (NN_NIL^{KN9204}/ NN_NIL^{J411})	*p*-adjusted	log_2FC (LN_NIL^{KN9204}/ LN_NIL^{J411})	*p*-adjusted	NR_description
Ethylene					
TraesCS1A02G370400	-5.05	0.0004	-2.53	5.63E-05	ethylene-responsive transcription factor ERF109-like
TraesCS1A02G370600	-3.55	4.19E-17	-1.44	8.02E-05	AP2 domain containing protein
TraesCS1A02G370700	-5.28	1.08E-51	-2.08	8.05E-11	ethylene-responsive transcription factor ERF109-like
TraesCS1B02G117400	-1.32	5.13E-05	-1.44	6.19E-09	1-aminocyclopropane-1-carboxylate oxidase-like
TraesCS1B02G389700	-3.15	3.17E-20	-1.49	6.98E-06	ethylene responsive transcription factor 6
TraesCS1B02G389800	-3.64	1.61E-26	-1.78	1.94E-07	ethylene-responsive transcription factor ERF109-like
TraesCS1D02G098000	-1.80	2.67E-11	-1.77	5.13E-10	1-aminocyclopropane-1-carboxylate oxidase-like
TraesCS1D02G098100	-1.10	8.10E-06	-1.51	7.25E-09	1-aminocyclopropane-1-carboxylate oxidase-like
TraesCS1D02G376500	-4.11	8.13E-33	-1.79	7.68E-08	ethylene-responsive transcription factor ERF109-like
TraesCS1D02G376600	-3.26	2.22E-37	-1.33	0.0001	ethylene-responsive transcription factor ERF109-like
TraesCS1D02G376700	-3.34	1.30E-23	-1.36	2.22E-05	ethylene-responsive transcription factor ERF109-like
TraesCS1D02G376800	-4.79	1.53E-42	-2.08	0.0005	ethylene-responsive transcription factor ERF109-like
TraesCS2D02G397100	-5.47	0.0002	-2.92	4.59E-09	ethylene-responsive transcription factor ERF025-like
TraesCS3B02G158800	1.56	0.037	1.89	0.003	AP2 domain transcription factor TaDREB2
TraesCS3B02G412500	-2.39	4.76E-05	-1.17	0.046	F-box domain containing protein, expressed
TraesCS4A02G256500	-4.94	5.60E-08	-4.57	5.50E-19	1-aminocyclopropane-1-carboxylate synthase 1-like
TraesCS4B02G058200	-2.51	7.59E-09	-3.30	5.16E-23	1-aminocyclopropane-1-carboxylate synthase 1-like
TraesCS4D02G058200	-2.67	1.16E-12	-2.89	1.08E-23	1-aminocyclopropane-1-carboxylate synthase 1-like
TraesCS4D02G096400	-1.62	8.07E-10	-1.25	2.91E-11	lipase-like PAD4
TraesCS5B02G236900	-2.68	6.45E-17	-1.25	0.0009	ethylene-responsive transcription factor ERF109-like
TraesCS5D02G245300	-2.37	2.30E-10	-1.34	0.002	ethylene-responsive transcription factor ERF109-like
TraesCS6A02G235100	1.95	5.71E-07	1.08	0.004	predicted protein

(Continued)

TABLE 4 Continued

Gene_ ID	log_2FC (NN_NIL^{KN9204}/ NN_NIL^{J411})	*p*-adjusted	log_2FC (LN_NIL^{KN9204}/ LN_NIL^{J411})	*p*-adjusted	NR_description
TraesCS6A02G256600	-3.44	9.28E-14	-2.30	4.23E-12	ethylene-responsive transcription factor ERF027-like
TraesCS6A02G319500	-3.88	2.62E-11	-2.36	1.01E-09	ethylene-responsive transcription factor ERF109-like
TraesCS6A02G330500	-1.83	5.11E-16	-1.26	1.25E-06	ethylene-responsive transcription factor ERF014-like
TraesCS6B02G268700	-3.01	3.89E-17	-2.22	1.77E-19	ethylene-responsive transcription factor ERF027-like
TraesCS6B02G281000	-1.76	4.23E-09	-1.36	1.78E-07	ethylene-responsive transcription factor 1-like
TraesCS6B02G350100	-4.04	9.00E-12	-2.71	5.23E-10	ethylene-responsive transcription factor ERF109-like
TraesCS6B02G350400	-3.41	7.85E-42	-1.71	5.20E-07	ethylene-responsive transcription factor ERF109-like
TraesCS6B02G361400	-2.21	9.84E-22	-1.05	9.84E-08	ethylene-responsive transcription factor ERF014-like
TraesCS6D02G217800	1.72	1.14E-05	1.02	0.0004	ethylene-responsive transcription factor ERF054-like
TraesCS6D02G237800	-3.23	2.79E-19	-2.32	1.03E-21	ethylene-responsive transcription factor ERF027-like
TraesCS6D02G298700	-3.68	1.54E-06	-2.41	3.40E-09	ethylene-responsive transcription factor ERF109-like
TraesCS6D02G299000	-4.6422	0.007	-2.09	0.0022	ethylene-responsive transcription factor ERF109-like
TraesCS6D02G299100	-3.71	2.77E-37	-1.96	2.11E-06	ethylene-responsive transcription factor ERF109-like
TraesCS6D02G309600	-1.66	1.08E-15	-1.13	3.56E-05	ethylene-responsive transcription factor ERF014-like
Glutathione S-transferase					
TraesCS1B02G194100	-1.22	0.002	-1.11	0.0006	putative glutathione S-transferase GSTU6
TraesCS1B02G194500	-1.36	0.0005	-1.25	0.046	probable glutathione S-transferase GSTU6
TraesCS2A02G218700	-4.72	9.96E-19	-2.78	5.22E-20	probable glutathione S-transferase GSTU6
TraesCS2B02G244100	-3.87	3.27E-19	-2.39	6.06E-19	probable glutathione S-transferase GSTU6
TraesCS2B02G322800	-1.38	1.14E-06	-1.19	9.82E-05	glutathione S-transferase TCHQD
TraesCS2D02G044100	-3.99	0.03	-2.58	0.002	probable glutathione S-transferase GSTF1
TraesCS2D02G224700	-1.83	0.001	-1.72	5.55E-08	probable glutathione S-transferase GSTU6
TraesCS2D02G304500	-1.58	9.35E-06	-1.45	8.40E-12	glutathione S-transferase TCHQD
TraesCS3A02G309100	-1.92	5.18E-06	-1.14	4.15E-05	unnamed protein product
TraesCS3D02G130700	1.39	0.006	1.16	0.0006	probable glutathione S-transferase GSTU6
TraesCS3D02G486100	-1.15	9.69E-05	-1.07	3.18E-07	glutathione transferase GST 23-like
Gibberellin					
TraesCS1A02G334400	-1.81	2.73E-09	-2.32	3.52E-16	gibberellin 2-oxidase
TraesCS2A02G189600	-1.61	3.52E-11	-1.29	5.11E-09	chitin-inducible gibberellin-responsive protein 2-like
TraesCS2B02G217500	-1.59	8.03E-14	-1.32	1.55E-09	chitin-inducible gibberellin-responsive protein 2-like
TraesCS2B02G239400	-1.24	5.27E-08	-1.03	3.57E-05	chitin-inducible gibberellin-responsive protein 1
TraesCS2D02G198200	-1.36	5.50E-11	-1.46	1.23E-10	chitin-inducible gibberellin-responsive protein 2-like
TraesCS2D02G220200	-1.33	2.10E-10	-1.03	9.21E-07	chitin-inducible gibberellin-responsive protein 1
TraesCS3A02G122600	1.25	0.04	1.67	3.54E-07	gibberellin 3-oxidase 2-1
TraesCS3A02G294000	-1.73	2.71E-09	-1.45	9.93E-17	gibberellin 2-oxidase
TraesCS3B02G328700	-1.86	1.62E-08	-1.71	3.62E-07	gibberellin 2-oxidase 3 isozyme B1
TraesCS6A02G221900	-2.35	1.36E-13	-2.00	1.46E-10	gibberellin-2-oxidase-A9
TraesCS6D02G213100	-2.84	2.58E-08	-3.35	3.80E-17	gibberellin 2-beta-dioxygenase 8-like
Brassinosteroid					
TraesCS2A02G142300	1.42	4.85E-05	1.077	7.91E-05	probable cytochrome P450 313a4
TraesCS3B02G550900	-2.31	0.004	-1.70	0.0004	protein BRASSINOSTEROID INSENSITIVE 1-like isoform X1
TraesCS5B02G174400	1.24	9.18E-07	1.43	1.95E-07	receptor-like protein kinase BRI1-like 3
TraesCS5D02G181500	1.32	1.42E-07	1.56	4.46E-14	receptor-like protein kinase BRI1-like 3
Auxin					
TraesCS2A02G183900	-1.73	1.42E-12	-1.43	1.77E-13	probable indole-3-acetic acid-amido synthetase GH3.8
TraesCS5A02G378300	1.42	0.0498	1.12	3.10E-05	Auxin-responsive protein IAA30

(Continued)

TABLE 4 Continued

Gene_ ID	log_2FC (NN_NIL^{KN9204}/ NN_NIL^{J411})	*p*-adjusted	log_2FC (LN_NIL^{KN9204}/ LN_NIL^{J411})	*p*-adjusted	NR_description
TraesCS6B02G359400	-1.38	0.001	-1.07	0.005	predicted protein, partial
Cytokinin					
TraesCS1A02G156100	-3.19	2.83E-07	-2.22	3.79E-14	probable cytokinin riboside 5'-monophosphate phosphoribohydrolase LOGL10 isoform X1
TraesCS3D02G475800	-2.54	4.52E-07	-1.43	6.95E-05	cytokinin dehydrogenase 4-like

NN and LN indicate normal- and low-nitrogen conditions, respectively. AA and BB indicate the NIL^{KN9204} and the NIL^{J411}, respectively. The expression levels between the NIL^{KN9204} and the NIL^{J411} were compared under each condition, with the latter as a control. The expression ratios are presented as log_2FC values. Genes with a $log_2FC \leq -1$ (p-adjusted< 0.05, coloured blue) represent the genes whose expression was downregulated in the NIL^{KN9204}, and genes with $log_2FC \geq 1$ (p-adjusted< 0.05, coloured red) represent the genes whose expression was upregulated in the NIL^{KN9204}.

TABLE 5 Differentially expressed TF-encoding genes between the pairwise NILs.

Gene_ ID	log_2FC (NN_NIL^{KN9204}/ NN_NIL^{J411})	*p*-adjusted	log_2FC (LN_NIL^{KN9204}/ LN_NIL^{J411})	*p*-adjusted	NR_description
NTF					
TraesCS1A02G354900	0.70	1	2.16	0.02	nuclear transcription factor Y subunit C-3-like
TraesCS1B02G366800	0.64	0.89	1.83	0.0007	nuclear transcription factor Y subunit C-3-like
TraesCS1D02G355600	0.45	0.95	2.60	0.003	nuclear transcription factor Y subunit C-3-like
NAC					
TraesCS3A02G078400	1.48	0.004	1.37	3.04E-07	NAC transcription factor
TraesCS3A02G339600	-3.07	3.15E-22	-3.01	1.27E-27	NAC transcription factor 4
TraesCS3D02G078900	1.79	6.26E-06	1.39	5.36E-05	NAC transcription factor

NN and LN indicate normal- and low-nitrogen conditions, respectively. AA and BB indicate the NIL^{KN9204} and the NIL^{J411}, respectively. The expression levels between the NIL^{KN9204} and the NIL^{J411} were compared under each condition, with the latter as a control. The expression ratios are presented as log_2FC values. Genes with a $log_2FC \leq -1$ (p-adjusted< 0.05, coloured blue) represent the genes whose expression was downregulated in the NIL^{KN9204}, and genes with $log_2FC \geq 1$ (p-adjusted< 0.05, coloured red) represent the genes whose expression was upregulated in the NIL^{KN9204}.

TFs function in response to NO_3^-, depending on the NRT1.1 NO_3^- transport function (Vidal et al., 2014), to increase root biomass (He et al., 2015). Two genes encoding NAC TFs (*TraesCS3A02G078400* and *TraesCS3D02G078900*) exhibited higher expression levels in the NIL^{KN9204} than in the NIL^{J411} under both NN and LN conditions (Table 5), implying that they had similar effects on root growth. Ethylene responsive factors (ERFs) belong to the AP2/ERF (APETALA2/ERF) superfamily of transcription factors associated with various developmental processes and stress tolerance. It was reported that ERF transcription factor gene *TaSRL1* resulted in short root length when ectopically expressed in rice (Zhuang et al., 2021). In the present study, expressions of ERF-like genes were significantly down-regulated in the NIL^{KN9204} compared to the NIL^{J411} under both NN and LN conditions, which may contribute to longer root length in NIL^{KN9204}.

In conclusion, transcriptomic analysis in the present study revealed the landscape of the DEGs between the *QMrl-7B* NILs under both NN and LN conditions, reflecting the physiological basis of the large roots of the superior parent KN9204. This study used pairwise NILs for analysis to dampen the effects from different genetic backgrounds; as such, the DEGs are more likely to be related to *QMrl-7B*, either directly or indirectly. These results revealed many pathways regulated by genes that might interact genetically with *QMrl-7B*, which may provide a foundation for the application of *QMrl-7B* in molecular breeding. However, since the materials used for RNA-seq were seedlings and not mature plants, much work is still needed to elucidate the overall genetic network that controls ideal root traits of wheat plants at different stages.

Data availability statement

The data presented in the study are deposited in the NCBI repository, accession number PRJNA889686. The accession number PRJNA889686 (http://www.ncbi.nlm.nih.gov/bioproject/889686).

Author contributions

LS, JJL, LZ, NZ, WZ, DM, XR, JJ and JML conducted the hydroponic culture and field experiments. LS, JJL, LZ and AB analyzed the data. LS, JJL, YN and AB wrote the manuscript. RL and JML revised the manuscript. All authors contributed to the article and approved the submitted version.

Funding

This research was jointly supported by grants from the National Key Research and Development Program of China (2021YFF1000403), the National Natural Science Foundation of China (U22A6009), Hebei Natural Science Foundation (C2021205013) and China Agriculture Research System of MOF and MARA (CARS-03).

Acknowledgments

We are very grateful to Dr. Xigang Liu from Hebei Normal University, Shijiazhuang, China for his critical review of the manuscript.

Conflict of interest

The authors declare that the research was conducted in the absence of any commercial or financial relationships that could be construed as a potential conflict of interest.

Publisher's note

All claims expressed in this article are solely those of the authors and do not necessarily represent those of their affiliated organizations, or those of the publisher, the editors and the reviewers. Any product that may be evaluated in this article, or claim that may be made by its manufacturer, is not guaranteed or endorsed by the publisher.

Supplementary material

The Supplementary Material for this article can be found online at: https://www.frontiersin.org/articles/10.3389/fpls.2022.1062575/full#supplementary-material

References

An, D., Su, J., Liu, Q., Zhu, Y., Tong, Y., Li, J., et al. (2006). Mapping QTLs for nitrogen uptake in relation to the early growth of wheat (Triticum aestivum l.). *Plant Soil.* 284, 73–84. doi: 10.1007/s11104-006-0030-3

Appels, R., Eversole, K., Feuillet, C., Keller, B., Rogers, J., Stein, N., et al. (2018). Shifting the limits in wheat research and breeding using a fully annotated reference genome. *Science* 361, eaar7191. doi: 10.1126/science.aar7191

Cao, P., Ren, Y., Zhang, K., Teng, W., Zhao, X., Dong, Z., et al. (2014). Further genetic analysis of a major quantitative trait locus controlling root length and related traits in common wheat. *Mol. Breeding.* 33, 975–985. doi: 10.1007/s11032-013-0013-z

Chen, D., Richardson, T., Chai, S., Lynne McIntyre, C., Rae, A. L., and Xue, G. P. (2016). Drought-UP-REGULATED TaNAC69-1 is a transcriptional repressor of TaSHY2 and TaIAA7, and enhances root length and biomass in wheat. *Plant Cell Physiol.* 57, 2076–2090. doi: 10.1093/pcp/pcw126

Chen, H., Wei, J., Tian, R., Zeng, Z., Tang, H., Liu, Y., et al. (2022). A major quantitative trait locus for wheat total root length associated with precipitation distribution. *Front. Plant Sci.* 13. doi: 10.3389/fpls.2022.995183

Cosio, C., and Dunand, C. (2009). Specific functions of individual class III peroxidase genes. *J. Exp. Bot.* 60, 391–408. doi: 10.1093/jxb/ern318

Dalal, M., Sahu, S., Tiwari, S., Rao, A., and Gaikwad, K. (2018). Transcriptome analysis reveals interplay between hormones, ROS metabolism and cell wall biosynthesis for drought-induced root growth in wheat. plant physiol. *Biochem.* 130, 482–492. doi: 10.1016/j.plaphy.2018.07.035

Ding, X., Cao, Y., Huang, L., Zhao, J., Xu, C., Li, X., et al. (2008). Activation of the indole-3-acetic acid-amido synthetase GH3-8 suppresses expansin expression and promotes salicylate- and jasmonate-independent basal immunity in rice. *Plant Cell.* 20, 228–240. doi: 10.1105/tpc.107.055657

Fan, X., Zhang, W., Zhang, N., Chen, M., Zheng, S., Zhao, C., et al. (2018). Identification of QTL regions for seedling root traits and their effect on nitrogen use efficiency in wheat (Triticum aestivum l.). *Theor. Appl. Genet.* 131, 2677–2698. doi: 10.1007/s00122-018-3183-6

Fukaki, H., and Tasaka, M. (2009). Hormone interactions during lateral root formation. *Plant Mol. Biol.* 69, 437–449. doi: 10.1007/s11103-008-9417-2

Gelli, M., Duo, Y., Konda, A., Zhang, C., Holding, D., and Dweikat, I. (2014). Identification of differentially expressed genes between sorghum genotypes with contrasting nitrogen stress tolerance by genome-wide transcriptional profiling. *BMC Genomics* 15, 179. doi: 10.1186/1471-2164-15-179

Gewin, V. (2010). Food: An underground revolution. *Nature.* 466, 552–553. doi: 10.1038/466552a

Godfray, H. C., Beddington, J. R., Crute, I. R., Haddad, L., Lawrence, D., Muir, J. F., et al. (2010). Food security: the challenge of feeding 9 billion people. *Science.* 327, 812–818. doi: 10.1126/science.1185383

Gou, J., Strauss, S. H., Tsai, C. J., Fang, K., Chen, Y., Jiang, X., et al. (2010). Gibberellins regulate lateral root formation in populus through interactions with auxin and other hormones. *Plant Cell.* 22, 623–639. doi: 10.1105/tpc.109.073239

Guo, R., Hu, Y., Aoi, Y., Hira, H., Ge, C., Dai, X., et al. (2022). Local conjugation of auxin by the GH3 amido synthetases is required for normal development of roots and flowers in arabidopsis. *Biochem. Biophys. Res. Commun.* 589, 16–22. doi: 10.1016/j.bbrc.2021.11.109

Han, Y., Gao, Y., Shi, Y., Du, J., Zheng, D. , and Liu, G. (2017b). Genome-wide transcriptome profiling reveals the mechanism of the effects of uniconazole on root development in glycine max. *J. Plant Biol.* 60, 387–403. doi: 10.1007/s12374-017-0028-9

Han, H., Wang, H., Han, Y., Hu, Z., Xin, M. , Peng, H., et al. (2017a). Altered expression of the TaRSL2 gene contributed to variation in root hair length during allopolyploid wheat evolution. *Planta.* 246, 1019–1028. doi: 10.1007/s00425-017-2735-3

Hao, L., Wen, Y., Zhao, Y., Lu, W., and Xiao, K. (2015). Wheat mitogen-activated protein kinase gene TaMPK4 improves plant tolerance to multiple stresses through modifying root growth, ROS metabolism, and nutrient acquisitions. *Plant Cell Rep.* 34, 2081–2097. doi: 10.1007/s00299-015-1853-2

He, X., Ma, H., Zhao, X., Nie, S., Li, Y., Zhang, Z., et al. (2016). Comparative RNA-seq analysis reveals that regulatory network of maize root development controls the expression of genes in response to n stress. *PloS One* 11, e0151697. doi: 10.1371/journal.pone.0151697

He, X., Qu, B., Li, W., Zhao, X., Teng, W., Ma, W., et al. (2015). The nitrate-inducible NAC transcription factor TaNAC2-5A controls nitrate response and increases wheat yield. *Plant Physiol.* 169, 1991–2005. doi: 10.1104/pp.15.00568

Ho, C. H., Lin, S. H., Hu, H. C., and Tsay, Y. F. (2009). CHL1 functions as a nitrate sensor in plants. *Cell.* 138, 1184–1194. doi: 10.1016/j.cell.2009.07.004

Hu, L., Li, H., Chen, L., Lou, Y., Amombo, E., and Fu, J. (2015). RNA-Seq for gene identification and transcript profiling in relation to root growth of bermudagrass (Cynodon dactylon) under salinity stress. *BMC Genomics* 16, 575. doi: 10.1186/s12864-015-1799-3

Hu, Z., Wang, R., Zheng, M., Liu, X., Meng, F., Wu, H., et al. (2018). TaWRKY51 promotes lateral root formation through negative regulation of ethylene biosynthesis in wheat (Triticum aestivum l.). *Plant J.* 96, 372–388. doi: 10.1111/tpj.14038

Kabir, M. R., Liu, G., Guan, P., Wang, F., Khan, A. A., Ni, Z., et al. (2015). Mapping QTLs associated with root traits using two different populations in wheat (Triticum aestivum l.). *Euphytica.* 206, 175–190. doi: 10.1007/s10681-015-1495-z

Krouk, G., Lacombe, B., Bielach, A., Perrine-Walker, F., Malinska, K., Mounier, E., et al. (2010). Nitrate-regulated auxin transport by NRT1.1 defines a mechanism for nutrient sensing in plants. *Dev. Cell.* 18, 927–937. doi: 10.1016/j.devcel.2010.05.008

Kücke, M., Schmid, H., and Spiess, A. (1995). A comparison of four methods for measuring roots of field crops in three contrasting soils. *Plant Soil.* 172, 63–71. doi: 10.1007/BF00020860

Kurakawa, T., Ueda, N., Maekawa, M., Kobayashi, K., Kojima, M., Nagato, Y., et al. (2007). Direct control of shoot meristem activity by a cytokinin-activating enzyme. *Nature.* 445, 652–655. doi: 10.1038/nature05504

Li, B., Liu, D., Li, Q., Mao, X., Li, A., Wang, J., et al. (2016). Overexpression of wheat gene TaMOR improves root system architecture and grain yield in oryza sativa. *J. Exp. Bot.* 67, 4155–4167. doi: 10.1093/jxb/erw193

Li, H., Torres-Garcia, J., Latrasse, D., Benhamed, M., Schilderink, S., Zhou, W., et al. (2017). Plant-specific histone deacetylases HDT1/2 regulate GIBBERELLIN 2-OXIDASE2 expression to control arabidopsis root meristem cell number. *Plant Cell.* 29, 2183–2196. doi: 10.1105/tpc.17.00366

Liu, H., Wang, Z., Xu, W., Zeng, J., Li, L., Li, S., et al. (2020). Bacillus pumilus LZP02 promotes rice root growth by improving carbohydrate metabolism and phenylpropanoid biosynthesis. *Mol. Plant Microbe Interact.* 33, 1222–1231. doi: 10.1094/mpmi-04-20-0106-r

Liu, J., Zhang, Q., Meng, D., Ren, X., Li, H., Su, Z., et al. (2021). QMrl-7B enhances root system, biomass, nitrogen accumulation and yield in bread wheat. *Plants.* 10, 764. doi: 10.3390/plants10040764

Li, C., Wang, J., Li, L., Li, J., Zhuang, M., Li, B., et al. (2022). TaMOR is essential for root initiation and improvement of root system architecture in wheat. *Plant Biotechnol. J.* 20, 862–875. doi: 10.1111/pbi.13765

Love, M. I., Huber, W., and Anders, S. (2014). Moderated estimation of fold change and dispersion for RNA-seq data with DESeq2. *Genome Biol.* 15 (12), 550. doi: 10.1186/s13059-014-0550-8

Lynch, J. (2007). Roots of the second green revolution. *Aust. J. Bot.* 55, 493–512. doi: 10.1071/BT06118

Maccaferri, M., El-Feki, W., Nazemi, G., Salvi, S., Canè, M. A., Colalongo, M. C., et al. (2016). Prioritizing quantitative trait loci for root system architecture in tetraploid wheat. *J. Exp. Bot.* 67, 1161–1178. doi: 10.1093/jxb/erw039

Maqbool, S., Hassan, M. A., Xia, X., York, L. M., Rasheed, A., and He, Z. (2022).). root system architecture in cereals: progress, challenges and perspective. *Plant J.* 110, , 23–, 42. doi: 10.1111/tpj.15669

Meister, R., Rajani, M. S., Ruzicka, D., and Schachtman, D. P. (2014). Challenges of modifying root traits in crops for agriculture. *Trends Plant Sci.* 19, 779–788. doi: 10.1016/j.tplants.2014.08.005

Merchuk-Ovnat, L., Fahima, T., Ephrath, J. E., Krugman, T., and Saranga, Y. (2017). Ancestral QTL alleles from wild emmer wheat enhance root development under drought in modern wheat. *Front. Plant Sci.* 8. doi: 10.3389/fpls.2017.00703

Moubayidin, L., Mambro, R. D., and Sabatini, S. (2009). Cytokinin-auxin crosstalk. *Trends Plant Sci.* 14, , 557–, 562. doi: 10.1016/j.tplants.2009.06.010

Muro-Villanueva, F., Mao, X., and Chapple, C. (2019). Linking phenylpropanoid metabolism, lignin deposition, and plant growth inhibition. *Curr. Opin. Biotechnol.* 56, 202–208. doi: 10.1016/j.copbio.2018.12.008

Neogy, A., Singh, Z., Mushahary, K., and Yadav, S. (2021). Dynamic cytokinin signaling and function of auxin in cytokinin responsive domains during rice crown root development. *Plant Cell Rep.* 40, 1367–1375. doi: 10.1007/s00299-020-02618-9

Pattyn, J., Vaughan-Hirsch, J., and Poel, B. (2020). The regulation of ethylene biosynthesis: a complex multilevel control circuitry. *New Phytol.* 229, 770–782. doi: 10.1111/nph.16873

Qu, B., He, X., Wang, J., Zhao, Y., Teng, W., Shao, A., et al. (2015). A wheat CCAAT box-binding transcription factor increases the grain yield of wheat with less fertilizer input. *Plant Physiol.* 167, 411–423. doi: 10.1104/pp.114.246959

Shi, X., Cui, F., Han, X., He, Y., Zhao, L., Zhang, N., et al. (2022). Comparative genomic and transcriptomic analyses uncover the molecular basis of high nitrogen-use efficiency in the wheat cultivar kenong 9204. *Mol. Plant* 15, 1440–1456. doi: 10.1016/j.molp.2022.07.008

Springmann, M., Clark, M., Mason-D'Croz, D., Wiebe, K., Bodirsky, B. L., Lassaletta, L., et al. (2018). Options for keeping the food system within environmental limits. *Nature.* 562, 519–525. doi: 10.1038/s41586-018-0594-0

Staswick, P. E., Serban, B., Rowe, M., Tiryaki, I., Maldonado, M. T., Maldonado, M. C., et al. (2005). Characterization of an arabidopsis enzyme family that conjugates amino acids to indole-3-acetic acid. *Plant Cell.* 17, 616–627. doi: 10.1105/tpc.104.026690

Tal, I., Zhang, Y., Jorgensen, M. E., Pisanty, O., Barbosa, I. C. R., Zourelidou, M., et al. (2016). The arabidopsis NPF3 protein is a GA transporter. *Nat. Commun.* 7, 11486. doi: 10.1038/ncomms11486

Vidal, E. A., Alvarez, J. M., and Gutierrez, R. A. (2014). Nitrate regulation of AFB3 and NAC4 gene expression in arabidopsis roots depends on NRT1.1 nitrate transport function. *Plant Signal. Behav.* 9, e28501. doi: 10.4161/psb.28501

Wang, R. F., An, D. G., Hu, C. S., Li, L. H., Zhang, Y. M., Jia, Y. G., et al. (2011). Relationship between nitrogen uptake and use efficiency of winter wheat grown in the north China plain. *Crop Pasture Sci.* 62, 504–514. doi: 10.1071/CP10383

Wang, Y., Cheng, Y., Chen, K. , and Tsay, Y. (2018b). Nitrate transport, signaling, and use efficiency. *Annu. Rev. Plant Biol.* 69, 85–122. doi: 10.1146/annurev-arplant-042817-040056

Wang, H., Hu, Z., Huang, K., Han, Y., Zhao, A. , Han, H., et al. (2018a). Three genomes differentially contribute to the seedling lateral root number in allohexaploid wheat: evidence from phenotype evolution and gene expression. *Plant J.* 95, 976–987. doi: 10.1111/tpj.14005

Wei, Z., and Li, J. (2016). Brassinosteroids regulate root growth, development, and symbiosis. *Mol. Plant* 9, 86–100. doi: 10.1016/j.molp.2015.12.003

Xu, G., Fan, X., and Miller, A. (2012). Plant nitrogen assimilation and use efficiency. *Annu. Rev. Plant Biol.* 63, 153–182. doi: 10.1146/annurev-arplant-042811-105532

Xu, Y., Ren, Y., Lin, T., and Cui, D. (2019). Identification and characterization of CircRNAs involved in the regulation of wheat root length. *Biol. Res.* 52, 19. doi: 10.1186/s40659-019-0228-5

Yang, J., Wang, M., Li, W., He, X., Teng, W., Ma, W., et al. (2019). Reducing expression of a nitrate-responsive bZIP transcription factor increases grain yield and n use in wheat. *Plant Biotechnol. J.* 17, 1823–1833. doi: 10.1111/pbi.13103

Zhang, H., and Forde, B. G. (1998). An arabidopsis MADS box gene that controls nutrient-induced changes in root architecture. *Science.* 279, 407–409. doi: 10.1126/science.279.5349.40

Zheng, Z., Guo, Y., Novák, O., Chen, W., Ljung, K., Noel, J., et al. (2016). Local auxin metabolism regulates environment-induced hypocotyl elongation. *Nat. Plants.* 2, 16025. doi: 10.1038/nplants.2016.25

Zheng, X., Wen, X., Qiao, L., Zhao, J., Zhang, X., Li, X., et al. (2019). A novel QTL QTrl.saw-2D.2 associated with the total root length identified by linkage and association analyses in wheat (Triticum aestivum l.). *Planta.* 250, 129–143. doi: 10.1007/s00425-019-03154-x

Zhuang, M., Li, C., Wang, J., Mao, X., Li, L., Yin, J., et al. (2021). The wheat SHORT ROOT LENGTH 1 gene TaSRL1 controls root length in an auxin-dependent pathway. *J. Exp. Bot.* 72, 6977–6989. doi: 10.1093/jxb/erab357